

High-bias conductance of atom-sized Al contacts

Jun-ichi Mizobata,* Akihiro Fujii, Shu Kurokawa, and Akira Sakai†

International Innovation Center, Kyoto University, Sakyo-ku, Kyoto 606-8501, Japan

(Received 10 May 2003; revised manuscript received 24 July 2003; published 28 October 2003)

We measured the high-bias conductance of atom-sized Al contacts at room temperature for biases from 0.1 to 0.8 V, and studied the formation probability and the lifetime of Al single-atom contacts (SACs) under high biases. Analyses of conductance plateaus corresponding to Al SACs revealed that the formation probability of SACs decreases with increasing the bias and leads to the suppression of the first peak in the conductance histogram. The formation probability vanishes at a critical bias $V_{bc} \sim 0.8$ V. On the other hand, the average plateau length, representing the average lifetime of SACs, decreases almost linearly with increasing the bias but remains finite at V_{bc} . Similar results were also obtained for Au SACs but with a higher critical bias $V_{bc} \sim 2.4$ V. We consider that the reduction of the formation probability of Al and Au SACs is due to a current-induced contact instability, which takes place before the contact is reduced to a SAC. On the other hand, the mechanism of the observed linear bias dependence of the SAC plateau length is yet unclarified.

DOI: 10.1103/PhysRevB.68.155428

PACS number(s): 81.07.Lk, 73.63.Rt, 73.40.Jn, 66.30.Qa

I. INTRODUCTION

In the past decade, a number of theoretical and experimental studies have been carried out on atom-sized metal contacts.¹ Among various atom-sized contacts, the simplest but most interesting contact is a single-atom contact (SAC), which connects two electrodes through a single atom or a single chain of atoms. Metal SACs have a high fracture toughness comparable to that of an ideal crystal^{2,3} and also show a characteristic conductance, which varies depending on a contact geometry and a valency of an atom occupying the single-atom contact site.⁴⁻⁷ For certain metals such as Au, Ag, Cu, and Al the conductance of their SACs tends to take a value close to one quantum unit of conductance $G_0 = 2e^2/h$.

In our previous experiments,^{8,9} we studied the high-bias conductance of Au SACs and found that they can be observed up to about 2 V. Also, measurements of I - V characteristics¹⁰ and the current-induced disruption experiments¹¹ confirmed that some Au SACs can survive up to 2.3 V and sustain a current of ~ 180 μ A. However, it is not yet well understood why Au SACs become unstable around 2 V. Recently, a bias/current-induced bond weakening^{12,13} has been theoretically predicted in Au SACs, but it has not yet been confirmed experimentally. To shed light on the high-bias instability of SACs, it would be helpful to investigate various metal SACs under high biases and compare their behaviors. In this work, we chose Al SACs as typical non-Au SACs, measured their high-bias conductance, and compared it with that of Au SACs.

There have been a number of theoretical investigations on the conductance of Al SACs,^{4,14-22} and various conductance values were obtained ranging from $0.8G_0$ to $1.6G_0$ depending on structural models employed in the conductance calculation. On the other hand, all previous experiments²³⁻²⁶ agree that the conductance of Al SACs is $\sim 0.8G_0$. No experimental information is, however, available at this time about the atomic arrangement of Al SACs. Hasmy *et al.*²⁷ carried out simulations of breaking Al nanocontacts and found that a couple of contact geometries are preferred just before the

contact break. Perhaps, these preferred SACs are responsible for the observed $0.8G_0$ conductance.

The high-bias conductance of an Al SAC was theoretically investigated by Kobayashi *et al.*¹⁹ who calculated the conductance of a straight three-atom chain of Al for biases up to 2 V. They showed that the conductance of this three-atom chain decreases by 7% when the bias increases from 0 to 2 V. Furuya *et al.*²¹ extended the bias range up to 10 V and found an onset of nonlinear I - V relations at around 3 V. Recently, Halbritter *et al.*²⁶ carried out detailed experimental studies of bias/current-induced effects on Al nanocontacts. They employed a MCB junction technique and investigated the dynamic evolution of the connective neck at 4.2 K for biases up to 0.4 V. By analyzing conductance fluctuations, they demonstrated significant effects of heat dissipation, current-enhanced diffusion, and electromigration, which lead to various kinds of contact instability at different stages of the contact deformation.

In most breaking-junction experiments, SACs are usually detected by monitoring a transient conductance while breaking a macroscopic contact. In the case of Al and Au, the formation of their SACs is signaled by a conductance plateau appearing around $1G_0$. The stability of SACs can, therefore, be studied by examining such conductance plateaus. Unfortunately, we have poor control over atomic-scale contact breaking processes at room temperature, and this makes the plateau formation a statistical event, not reproducible in every contact break. We therefore have to acquire a large number of transient conductance traces and obtain two statistical quantities, p and $\langle \tau \rangle$, which represent the formation probability of SAC plateaus and their average length, respectively. Another method is to construct a conductance histogram, where the conductance data of SAC plateaus accumulate to form a well-defined peak. The height of this peak is proportional to $p \times \langle \tau \rangle$. Stable contacts should have high p and/or high $\langle \tau \rangle$, and hence form a tall peak in the histogram. Therefore, by examining p and $\langle \tau \rangle$ as a function of the bias voltage, we can obtain some information on the stability of SACs under high biases. In our previous work on Au relay contacts,⁹ we studied p_{Au} and $\langle \tau_{\text{Au}} \rangle$ of Au SACs. In

this work, we investigated the bias dependence of p_{Al} and $\langle \tau_{\text{Al}} \rangle$ of Al SACs at room temperature for biases from 0.1 to 0.8 V. Some preliminary results have been reported in Ref. 28.

II. EXPERIMENT

We employed a “pin-plate” setup, similar to the one used by Landman *et al.*²⁹ A contact was formed and broken between a 0.5 mm Al wire and a 10 mm diameter Al disk, both of which are of 99.999% purity. The wire and the disk were lightly etched in a NaOH solution before introducing them into a vacuum chamber, but no further cleaning was made *in situ*. We moved the Al wire against the disk using a commercial STM approach module (Burleigh ARIS-10-0.5), which consists of an Inchworm piezo motor and a tubular PZT scanner. We used a “hard indentation” method for contact formation. As pointed out by Hansen *et al.*,¹⁰ the “hard indentation” of the wire into the disk breaks surface oxide layers and yields a fresh contact with less chance of contamination than a contact prepared by soft tip-sample touching. A contact was first made by crushing the wire against the disk until the contact resistance becomes less than 20Ω . The wire was further pushed against the sample by moving it $\approx 1\ \mu\text{m}$ and then pulled away from the sample. After reestablishing the contact again, the wire was moved forward by $\sim 12\ \text{nm}$. During these procedures, the tube scanner continued axial vibration at 1 Hz with an amplitude of 21 nm and after the final approach of the wire to the disk the wire-disk contact repeated on-offs at 1 Hz. We used a symmetrical triangular signal for driving the tube scanner, and the breaking speed of the contact was 42 nm/s. All measurements were carried out at room temperature in UHV better than $5 \times 10^{-8}\ \text{Pa}$. It usually took longer than 10 hrs to take all conductance data, so that the contamination might be a problem even in UHV. However, we found no significant difference between the conductance data taken at the beginning of the experiment and those at later times. We, therefore, believe that a fresh contact is always formed after each “hard indentation,” though we cannot completely rule out a possibility of fast reaction of a freshly born contact with residual gases.^{30–33}

We measured the transient conductance at each contact break by monitoring a voltage drop across a current-sensing resistor ($1\ \text{k}\Omega$) connected in series with the contact. A fast digital oscilloscope (Tektronix TDS3052; maximum sampling rate 5 GS/s, 350 MHz bandwidth) was used to record the voltage signal at a sampling rate of 25 MS/s or with a time interval of 40 ns. Since an applied voltage V_a on the whole circuit is divided by the contact and the current-sensing resistor, the true bias voltage V_b across the contact is not equal to V_a but depends on the conductance G of the contact through a relation $V_b = V_a / (1 + GR)$, where R denotes the resistance of the current-sensing resistor. At $G \sim 1G_0$, the difference between V_a and V_b is 7%.

Figure 1 shows an example of transient conductance trace observed in an Al contact at $V_a = 0.4\ \text{V}$. This trace displays two plateaus, a short plateau around $2G_0$ and a long one at $1G_0$. This latter plateau, like many other plateaus observed in Al contacts, exhibits an appreciable positive slope, in con-

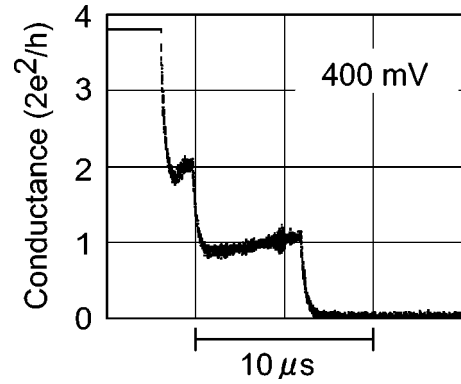


FIG. 1. A conductance trace of an Al nanocontact observed at $V_a = 0.4\ \text{V}$. Typical conductance trace of an Al breaking contact recorded at 400 mV. The conductance decreases stepwise and shows plateaus. A positive slope of plateaus, characteristic of Al, is evident in this trace.

trast to almost flat plateaus in Au contacts. This positive slope is a characteristic feature of Al plateaus and theoretically explained in terms of changes in the electronic structure of Al nanocontacts during their elastic deformation.^{16,17} For $V_a > 0.2\ \text{V}$, a considerable fraction of conductance traces showed an abrupt increase after they once dropped below $1.5G_0$, suggesting a momentary reformation of the contact. This chatteringlike phenomenon is perhaps the same contact instability as that reported by Halbritter *et al.*²⁶ Since many of such traces showed conductance plateaus during their initial breaking process, we did not discard these traces. At $V_a = 0.2\ \text{V}$, $\approx 20\%$ of traces show the abrupt conductance recovery, while the fraction increases to 44% at $V_a = 0.7\ \text{V}$. In Au contacts, the fraction is low and less than 25% for $V_a > 0.4\ \text{V}$. We will discuss this contact instability in Sec. IV in connection to the formation probability of SACs.

III. RESULTS

We carried out six conductance measurements on three different samples. The applied bias voltage was varied from 0.1 to 0.8 V by 0.1 V steps. At each bias, we obtained total 12 000 traces and used them to construct conductance histograms shown in Fig. 2. For $V_a \leq 0.4\ \text{V}$, histograms clearly exhibit a well-defined first conductance peak followed by smaller second and third peaks. The first peak locates slightly below $1G_0$ and appears more broadened compared to the sharp $1G_0$ peak of Au. These features of the low-bias conductance histograms are in good agreement with previous experiments.^{23,24,26} The broadening of the first peak is partly due to a positive slope of conductance plateaus, and partly attributed to a shoulderlike structure appearing at a low-conductance side of the first peak. This structure was more evident in some measurements but became a little obscured in histograms in Fig. 2, which were obtained by summing up the results of six measurements. Nevertheless, a shoulder of the first peak can be seen in histograms at $V_a = 0.5$ and $0.6\ \text{V}$. We note that the first peak in Fig. 6 in Ref. 26 also shows a similar shoulder structure. The authors of Ref. 26 even observed a splitting of the first peak in some conductance his-

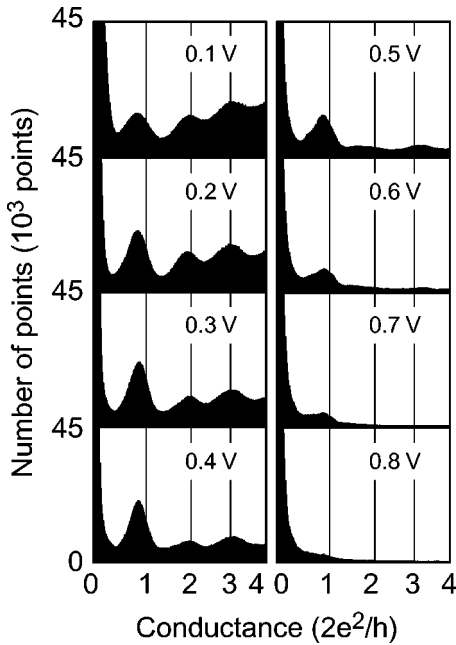


FIG. 2. Bias dependence of the Al conductance histogram for $V_a=0.1-0.8$ V. The first peak shows a shoulderlike structure in histograms at 0.6 and 0.7 V.

tograms at 0.4 V. These observations suggest that the broad first peak of Al is actually a double peak composed of two narrowly separating peaks, perhaps corresponding to two different SAC configurations as pointed out by Halbritter *et al.*²⁶ Atomic arrangements of these Al SACs are yet unknown.

For $V_a > 0.5$ V, the first peak in Fig. 2 decreases in height with increasing V_a and almost disappears at 0.8 V. To investigate the bias dependence of this first peak more quantitatively, we carried out a Gaussian fitting to the first peak in each histogram. Taking into account the double-peak structure of the first peak, we decomposed it into a main peak and a subpeak, and obtained the position and the height of the main peak as a function of the bias voltage. The results are shown in Fig. 3. In this figure, the peak position and the height are plotted against V_b , a true bias voltage which was

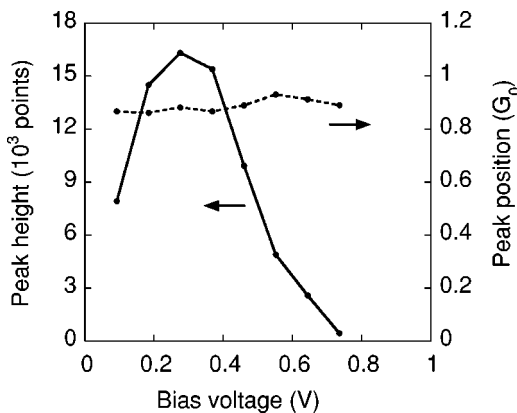


FIG. 3. Height and position of the first conductance peak as a function of V_b .

calculated from V_a using a relation mentioned in the preceding section. In Fig. 3, the peak position shows no appreciable shift with the bias and remains constant up to 0.8 V. We note that the same absence of peak shift was also observed for the $1G_0$ peak of Au and Au alloys under high biases.^{8,9,34} The result shown in Fig. 3 is also consistent with the weak bias dependence of the theoretical conductance of a three-atom Al SAC.²⁰ The average peak position is $(0.89 \pm 0.02)G_0$, which is about 11% higher than previously reported position ($0.8G_0$) of the first peak. This slight discrepancy is perhaps due to the double-peak structure of the first peak.

Contrary to the peak position, the peak height in Fig. 3 exhibits a strong bias dependence. It first increases with the bias, takes a maximum around 0.3 V, and then decreases rapidly for higher biases. The peak height vanishes at 0.8 V. This result is in marked contrast to the previous results on the $1G_0$ peak of Au, which can be observed up to 2 V.^{8,9} The low critical bias of the Al first peak clearly indicates low stability of Al SACs under high-bias/high-current conditions. To obtain further information on the contact stability, we estimated p and $\langle \tau \rangle$, the formation probability of SAC plateaus and their average length, respectively, by sampling SAC plateaus from 12 000 conductance traces. For discriminating genuine plateaus from conductance fluctuations due to noises, we selected such plateaus that have more than 10 data points, or spends longer than 400 ns, within a conductance window $(0.7-1.1)G_0$. Marginal plateaus shorter than 400 ns were hardly distinguishable from noises and were not taken into account. Our conductance window is much wider than that used in previous experiment⁹ for $1G_0$ plateaus of Au, but a wide window is necessary because Al plateaus have positive slopes as seen in Fig. 1. With the above criterion, we sorted out SAC plateaus from all conductance traces, counted the number n of them, and measured their length τ . We then obtained the formation probability p of SAC plateaus as $p = n/N$, where N is the total number of conductance traces recorded at each bias. As to the plateau length, we found that shorter plateaus appear more frequently than longer ones, and the distribution of τ can be well described by an exponential function. This exponential distribution of τ suggests that the plateau breaking would be a random event with a breaking rate $1/\langle \tau \rangle$, and $\langle \tau \rangle$ would represent the average lifetime of SAC plateaus. Note, however, that a possibility of Wigner distribution³⁵ cannot be ruled out since we could not detect plateaus shorter than 400 ns.

The p_{Al} and $\langle \tau_{Al} \rangle$ obtained by the above procedures are plotted as a function of the bias voltage V_b in Figs. 4 and 5, respectively. It can be seen in these plots that both p_{Al} and $\langle \tau_{Al} \rangle$ are bias dependent: they first increase with the bias, take a maximum around 0.3 V, and then decrease for $V_b > 0.3$ V. In this high bias regime, p_{Al} shows more rapid decrease than $\langle \tau_{Al} \rangle$ and almost vanishes at 0.8 V. On the other hand, $\langle \tau_{Al} \rangle$ decreases linearly with V_b but remains finite at 0.8 V. By comparing Fig. 3 with Fig. 4, it is evident that not $\langle \tau_{Al} \rangle$ but p_{Al} dominates the bias dependence of the first conductance peak height and leads to its suppression at $V_b > 0.3$ V. This situation is just the same as for the Au $1G_0$ peak, which is also suppressed by the reduction of p_{Au} under high biases.⁹ In the following section, we will compare p_{Al} and p_{Au} and discuss a mechanism of their reduction.

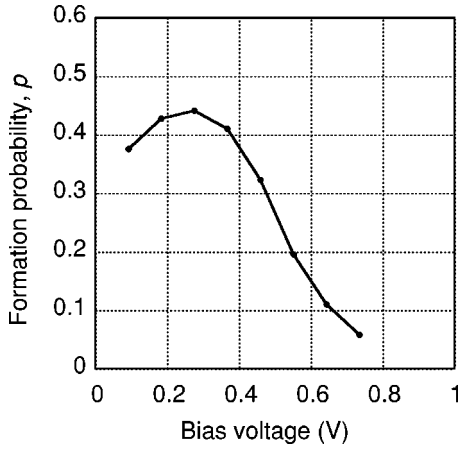


FIG. 4. Bias dependence of the formation probability p_{Al} of Al SACs.

IV. DISCUSSION

A. Formation probability of Al and Au SACs

We first discuss the observed bias dependence of p_{Al} by comparing it with that of p_{Au} . In our previous experiment on Au,⁹ we measured p_{Au} up to 2 V, but our old data cannot be compared with p_{Al} since they were taken on relay contacts in a gas atmosphere. Therefore, we remeasured p_{Au} in UHV and compared it with p_{Al} in Fig. 6. The p_{Au} extends up to 2.4 V, which is approximately three times higher than the critical bias (~ 0.8 V) of p_{Al} . Except this difference in the bias range, however, two plots in Fig. 6(a) exhibit similar bias dependence. This similarity becomes more evident when we plot p/p_{max} against V_b/V_{bc} , where V_{bc} is the critical bias at which p vanishes. In such a normalized plot, p_{Al} and p_{Au} are almost identical as shown in Fig. 6(b). This result clearly indicates that a common mechanism works for their bias-induced reduction.

Recently, García-Martín *et al.*³⁶ theoretically explained the bias dependence of $1G_0$ and $2G_0$ peak heights of Au reported in Ref. 9 in terms of nonlinear effects in conductance. According to their calculations, nonlinear effects scale with eV_b/E_F , where E_F is the Fermi energy. If the reduction of p_{Al} and p_{Au} is due to nonlinear effects, the ratio eV_{bc}/E_F

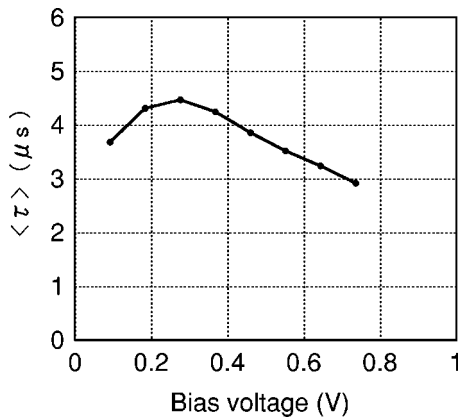


FIG. 5. Bias dependence of the average plateau length $\langle \tau_{Al} \rangle$ of Al SACs.

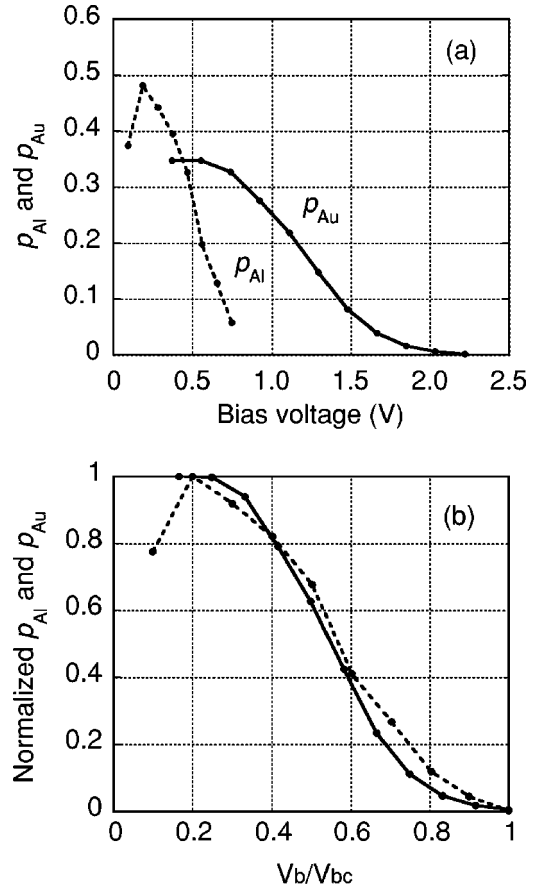


FIG. 6. Comparison of p_{Al} and p_{Au} (a) and their normalized plots (b) against V_b/V_{bc} .

is expected to be the same for Al and Au. The value of eV_{bc}/E_F of Al is, however, $\sim 1/6$ of that of Au. It thus seems that mechanisms other than the proposed nonlinear effects dominate the bias-induced suppression of p_{Al} and p_{Au} .

In Sec. II, we noted the chatteringlike behavior of the conductance of Al and Au nanocontacts under high biases. Similar unstable conductance was previously reported by Halbritter *et al.*²⁶ and also observed in Ag nanocontacts.³⁷ Our preliminary study indicated that this contact instability takes place when a contact current density reaches a certain critical value, or when a contact is reduced to a certain critical size, which corresponds to the conductance of $G \approx (10-50)G_0$. Since its onset depends on the current density, this contact instability is probably due to local melting or electromigration^{26,38-41} (perhaps, a massive electromigration involving many atoms, which may be indistinguishable from melting). Since the critical size is larger than the size of atoms and increases with the bias, the instability takes place before the contact is reduced to a SAC and hence suppresses the SAC formation. It is thus likely that this current-induced instability is the primary cause of the reduction of p under high biases. Since SACs are smaller than the critical contact size, they are unstable under high biases and considered to exist as metastable states, like a supersaturated solution. The probability of forming such metastable states is likely to be a certain universal function of the degree of supercriticality. If we assume that the ratio V_b/V_{bc} measures the degree of

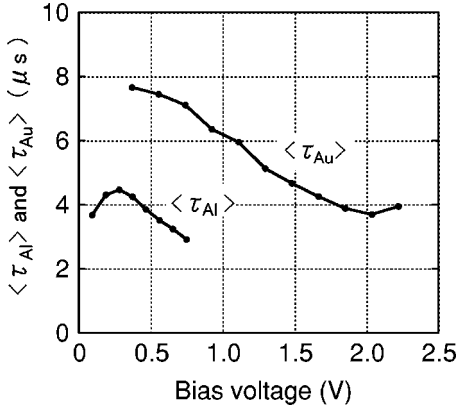


FIG. 7. Comparison of $\langle \tau_{Al} \rangle$ and $\langle \tau_{Au} \rangle$.

supercriticality of our metastable contacts, then we would be able to account for the observed universal reduction of p_{Al} and p_{Au} shown in Fig. 6(b), though we do not know the functional form of $p(V_b/V_{bc})$. We, however, have no clues at this time to understand why V_{bc} of p_{Au} is three times higher than that of p_{Al} . Our preliminary measurements³⁷ suggest that the critical current density of Au is higher than that of other metals, and this may be related to the observed high V_{bc} of Au.

B. Plateau length of Al and Au SACs

We next turn to $\langle \tau \rangle$ and compare $\langle \tau_{Al} \rangle$ and $\langle \tau_{Au} \rangle$ in Fig. 7. It can be seen that both $\langle \tau \rangle$ s exhibit a characteristic linear decrease with increasing the bias. They also appear to have the same slope, though the bias range is much different: the linear behavior of $\langle \tau_{Al} \rangle$ can be observed for $V_b \approx (0.3 - 0.8)$ V, while that of $\langle \tau_{Au} \rangle$ extends from 0.5 V up to around 2 V. At $V_b \gtrsim 2$ V, $\langle \tau_{Au} \rangle$ shows a saturating behavior. This apparent saturation is due to long $1G_0$ plateaus, which occasionally appear even at $V_b \sim V_{bc}$. Since p_{Au} becomes quite small near V_{bc} , even a small number of long plateaus can dominate $\langle \tau_{Au} \rangle$ and make it nearly constant. We note that the same saturating behavior of $\langle \tau_{Au} \rangle$ was previously observed on Au relay contacts for $V_b > 1.5$ V.⁹ It is not clear at this time whether these long plateaus observed near V_{bc} are genuine plateaus or caused by a stabilization of SACs by various contaminations,^{30-33,42} though the adsorption of foreign atoms or molecules seems less likely at high biases.⁴³ On the other hand, $\langle \tau_{Al} \rangle$ appears to show no such saturation and linearly decreases up to V_{bc} .

The observed $\langle \tau_{Al} \rangle$ and $\langle \tau_{Au} \rangle$ show that the mean lifetime of Al and Au SACs is the order of a few microsecond. Within this time interval, the Al wire moves only ~ 0.1 pm, which is three to four orders of magnitude smaller than the tip retraction (typically 0.1–1 nm) required for breaking SACs.^{2,44,45} This fact clearly indicates that Al and Au SACs under high biases are not ruptured by stress accumulation. If we assume that the elastic deformation rate of Al and Au SACs is not much different from the breaking speed (42 nm/s) of our contacts, and also use the observed stiffness of Au SACs,² then the increase in the deformation force during $\langle \tau \rangle$ is estimated to be ~ 1 pN, which is about three orders of magni-

tude smaller than the fracture strength (~ 1.5 nN) of a Au SAC.² Al and Au SACs are thus too short-lived to be ruptured by deformation.

We rather consider that certain high-bias/high-current effects determine the mean lifetime of Al and Au SACs. In his current-induced disruption experiments, Hansen¹¹ estimated that Au SACs at 2.3 V have a breaking rate of $\gtrsim 10^6$ Hz. The current-induced breaking should thus be a fast process, and the observed short $\langle \tau \rangle$ of a few microsecond may not be unreasonable. According to previous analyses of the Au plateau length,^{11,12} we can write $\langle \tau \rangle$ as

$$\langle \tau \rangle = \nu_0^{-1} \exp[E(V_b)/k_B T(V_b)], \quad (1)$$

where ν_0 is a frequency factor, and $E(V_b)$ and $T(V_b)$ are an activation energy, and a contact temperature respectively, both of which are considered to depend on the bias. Since $E(V_b)$ generally decreases and $T(V_b)$ increases with increasing the bias, $\langle \tau \rangle$ in Eq. (1) decreases at high biases. In order to go further with Eq. (1) and compare it with our experimental results in Fig. 7, however, we have to know how $E(V_b)$ and $T(V_b)$ change with the bias.

If SACs are broken at one of atomic bonds of the contact atom, then $E(V_b)$ would represent the bias-dependent bond energy of the contact atom. Recently, Todorov *et al.*¹² and Brandbyge *et al.*¹³ theoretically studied the bias/current-induced effects on the bond strength and found an appreciable bond weakening. For Au SACs, Todorov *et al.* obtained $E(V_b) = 0.738 - 0.14V_b$ eV, while Brandbyge *et al.* found a large reduction in the bond strength, which amounts to $\Delta F \approx (1 - 1.5)$ nN at 2 V, comparable to the breaking force of Au SACs. However, we found that these bond-weakening models of Au SACs, combined with Eq. (1), hardly reproduce the observed linear bias dependence of $\langle \tau_{Au} \rangle$ shown in Fig. 7. For $\langle \tau_{Al} \rangle$, we have no theoretical and experimental information on the current-induced bond weakening in Al SACs.

It is also difficult to obtain a reliable estimation of $T(V_b)$. According to the theoretical $T(V_b)$ by Todorov *et al.*,^{12,46} $T(V_b)$ is not much different from the ambient temperature when experiments are performed at 300 K. On the other hand, measurements of two-level fluctuations at low temperatures and at low biases^{47,48} indicate $T(V_b) = (0.1 - 0.5) eV_b/k_B$. If we extrapolate this relation up to 1 V, we would have $T(V_b) \approx (1200 - 5800)$ K, well above the melting point. On the other hand, an electron temperature of 1930 K was reported at room temperature on a $1G_0$ contact of Au at 1.5 V.⁴⁹ The value of $T(V_b)$ and its bias dependence are thus still a matter of controversy. Considering these uncertainties both in $E(V_b)$ and $T(V_b)$, it would be too early to analyze our experimental results with Eq. (1). Conversely, the observed $\langle \tau \rangle - V_b$ plots shown in Fig. 7 will hopefully be used to determine the bias dependence of $E(V_b)$ and $T(V_b)$.

The above discussion assumes that the fracture of SACs takes place at atomic bonds of the contact atom. Since the contact current concentrates to the contact atom, this seems to be a plausible assumption. However, our discussion on $p(V_b)$ leads to an idea that SACs under high biases are in metastable states against the current-induced instability. In

such metastable contacts, small structural fluctuations at a distant location from the contact site may trigger the contact instability and rupture the contact. Then, $\langle \tau \rangle$ would represent the incubation time for the nucleation of such fluctuations. It is, however, not clear at this time whether this new interpretation of $\langle \tau \rangle$ will lead to the observed linear bias dependence of $\langle \tau \rangle$ shown in Fig. 7.

V. CONCLUSIONS

In conclusion, we studied the high-bias conductance of Al SACs at room temperature and compared it with that of Au SACs. We found that the first peak in the conductance histogram, corresponding to the conductance of Al SACs, decreases in height with increasing the bias and disappears at 0.8 V. This critical bias is roughly one third of that of Au SACs. Except this difference in the magnitude of the critical bias, Al and Au SACs show similar bias dependence. The formation probabilities p_{Al} and p_{Au} of Al and Au SACs decrease to zero as the bias approaches the critical value and leads to the conductance peak suppression at high biases. Also, they exhibit the universal bias dependence. We consider that the current-induced contact instability, which takes place in the middle of the contact deformation, is responsible

for the reduction of p_{Al} and p_{Au} at high biases. However, it is not yet understood why Au has a higher critical bias and shows the superior resistance against the instability than Al. We also found that the average SAC plateau length, $\langle \tau_{\text{Al}} \rangle$ and $\langle \tau_{\text{Au}} \rangle$, decreases almost linearly with increasing the bias. This linear behavior of $\langle \tau_{\text{Al}} \rangle$ and $\langle \tau_{\text{Au}} \rangle$ appears incompatible with the Arrhenius-type formula for $\langle \tau \rangle$, but we cannot reach the conclusion since we lack reliable information about the bias dependence of the activation energy and the contact temperature.

Our experimental results on Al and Au SACs suggest that the high-bias behaviors of p and $\langle \tau \rangle$ are strongly related to the current-induced contact instability. Further high-bias experiments on other metals, e.g., Ag, Cu, Ni, Pd, and Pt, would be necessary to clarify the nature of this instability and understand the stability of metal SACs under high biases.

ACKNOWLEDGMENTS

This work was supported by the Grant-in-Aid for Scientific Research (B) Grant No. 14340091 from Japan Society for the Promotion of Science.

*Deceased.

†Corresponding author. Email address: sakai@iic.kyoto-u.ac.jp

¹N. Agraït, A. Levy Yeyati, and J.M. van Ruitenbeek, Phys. Rep. **377**, 81 (2003).

²G. Rubio-Bollinger, S.R. Bahn, N. Agraït, K.W. Jacobsen, and S. Vieira, Phys. Rev. Lett. **87**, 026101 (2001).

³S.R. Bahn and K.W. Jacobsen, Phys. Rev. Lett. **87**, 266101 (2001).

⁴J.C. Cuevas, A. Levy Yeyati, and A. Martín-Rodero, Phys. Rev. Lett. **80**, 1066 (1998).

⁵E. Scheer, P. Joyez, D. Esteve, C. Urbina, and M.H. Devoret, Phys. Rev. Lett. **78**, 18 (1997).

⁶E. Scheer, N. Agraït, J.C. Cuevas, A. Levy Yeyati, B. Ludoph, A. Martín-Rodero, G. Rubio-Bollinger, J.M. van Ruitenbeek, and C. Urbina, Nature (London) **395**, 780 (1998).

⁷T. López-Ciudad, A. García-Martín, A.J. Caamaño, and J.J. Sáenz, Surf. Sci. **440**, L887 (1999).

⁸H. Yasuda and A. Sakai, Phys. Rev. B **56**, 1069 (1997).

⁹K. Itakura, K. Yuki, S. Kurokawa, H. Yasuda, and A. Sakai, Phys. Rev. B **60**, 11 163 (1999).

¹⁰K. Hansen, S.K. Nielsen, M. Brandbyge, E. Lægsgaard, and F. Besenbacher, Appl. Phys. Lett. **77**, 708 (2000).

¹¹K. Hansen, Ph.D. thesis, Institute of Physics and Astronomy, University of Aarhus, Aarhus, 2000.

¹²T.N. Todorov, J. Hoekstra, and A.P. Sutton, Phys. Rev. Lett. **86**, 3606 (2001).

¹³M. Brandbyge, K. Stokbro, J. Taylor, J.-L. Mozos, and P. Ordejón, Phys. Rev. B **67**, 193104 (2003).

¹⁴N.D. Lang, Phys. Rev. B **52**, 5335 (1995).

¹⁵M. Heinemann and R.A. de Groot, Phys. Rev. B **55**, 9375 (1997).

¹⁶D. Sánchez-Portal, C. Untiedt, J.M. Soler, J.J. Sáenz, and N. Agraït, Phys. Rev. Lett. **79**, 4198 (1997).

¹⁷J.C. Cuevas, A. Levy Yeyati, A. Martín-Rodero, G. Rubio-

Bollinger, C. Untiedt, and N. Agraït, Phys. Rev. Lett. **81**, 2990 (1998).

¹⁸G. Taraschi, J.-L. Mozos, C.C. Wang, H. Guo, and J. Wang, Phys. Rev. B **58**, 13 138 (1998).

¹⁹N. Kobayashi, M. Brandbyge, and M. Tsukada, Phys. Rev. B **62**, 8430 (2000).

²⁰N. Kobayashi, M. Aono, and M. Tsukada, Phys. Rev. B **64**, 121402 (2001).

²¹S. Furuya, Y. Gohda, N. Sasaki, and S. Watanabe, Jpn. J. Appl. Phys., Part 2 **41**, L989 (2002).

²²T. Ono, Y. Fujimoto, and K. Hirose, Appl. Phys. Lett. **82**, 4570 (2003).

²³A.I. Yanson and J.M. van Ruitenbeek, Phys. Rev. Lett. **79**, 2157 (1997).

²⁴B. Ludoph and J.M. van Ruitenbeek, Phys. Rev. B **61**, 2273 (2000).

²⁵M. Díaz, J.L. Costa-Krämer, P.A. Serena, E. Medina, and A. Hasmy, Nanotechnology **12**, 118 (2001).

²⁶A. Halbritter, Sz. Csonka, O.Yu. Kolesnychenko, G. Mihály, O.I. Shklyarevskii, and H. van Kempen, Phys. Rev. B **65**, 045413 (2002).

²⁷A. Hasmy, E. Medina, and P.A. Serena, Phys. Rev. Lett. **86**, 5574 (2001).

²⁸J. Mizobata, A. Fujii, S. Kurokawa, and A. Sakai, Jpn. J. Appl. Phys. Part 1 **42**, 4680 (2003).

²⁹U. Landman, W.D. Luedtke, B.E. Salisbury, and R.L. Whetten, Phys. Rev. Lett. **77**, 1362 (1996).

³⁰S.R. Bahn, N. Lopez, J.K. Nørskov, and K.W. Jacobsen, Phys. Rev. B **66**, 081405 (2002).

³¹S.B. Legoas, D.S. Galvão, V. Rodrigues, and D. Ugarte, Phys. Rev. Lett. **88**, 076105 (2002).

³²S.K. Nielsen, M. Brandbyge, K. Hansen, K. Stokbro, J.M. van Ruitenbeek, and F. Besenbacher, Phys. Rev. Lett. **89**, 066804 (2002).

- ³³F.D. Novacs, A.J.R. da Silva, E.Z. da Silva, and A. Fazzio, *Phys. Rev. Lett.* **90**, 036101 (2003).
- ³⁴A. Enomoto, S. Kurokawa, and A. Sakai, *Phys. Rev. B* **65**, 125410 (2002).
- ³⁵J.L. Costa-Krämer, N. García, P. García-Mochales, P.A. Serena, M.I. Marqués, and A. Correia, *Phys. Rev. B* **55**, 5416 (1997).
- ³⁶A. García-Martín, M. del Valle, J.J. Sáenz, J.L. Costa-Krämer, and P.A. Serena, *Phys. Rev. B* **62**, 11 139 (2000).
- ³⁷A. Fujii, S. Kurokawa, and A. Sakai (unpublished).
- ³⁸T. Schmidt, R. Martel, R.L. Sandstrom, and Ph. Avouris, *Appl. Phys. Lett.* **73**, 2173 (1998).
- ³⁹H. Park, A.K.L. Lim, A.P. Alivisatos, J. Park, and P.L. McEuen, *Appl. Phys. Lett.* **75**, 301 (1999).
- ⁴⁰T.N. Todorov, J. Hoekstra, and A.P. Sutton, *Philos. Mag. B* **80**, 421 (2000).
- ⁴¹J.W.T. Heemskerk, Y. Noat, D.J. Bakker, J.M. van Ruitenbeek, B.J. Thijsse, and P. Klever, *Phys. Rev. B* **67**, 115416 (2003).
- ⁴²C. Shu, C.Z. Li, H.X. He, A. Bogozi, J.S. Bunch, and N.J. Tao, *Phys. Rev. Lett.* **84**, 5196 (2000).
- ⁴³Sz. Csonka, A. Halbritter, G. Mihály, E. Jurdik, O.I. Shklyarevskii, and H. van Kempen, *Phys. Rev. Lett.* **90**, 116803 (2003).
- ⁴⁴A.I. Yanson, G. Rubio-Bollinger, H.E. van den Brom, N. Agrait, and J.M. van Ruitenbeek, *Nature (London)* **395**, 783 (1998).
- ⁴⁵R.H.M. Smit, C. Untiedt, A.I. Yanson, and J.M. van Ruitenbeek, *Phys. Rev. Lett.* **87**, 266102 (2001).
- ⁴⁶T.N. Todorov, *Philos. Mag. B* **77**, 965 (1998).
- ⁴⁷P.A.M. Holweg, J. Caro, A.H. Verbruggen, and S. Radelaar, *Phys. Rev. B* **45**, 9311 (1992).
- ⁴⁸H.E. van den Brom, Ph.D. thesis, Universiteit Leiden, The Netherlands, 2000.
- ⁴⁹A. Downes, Ph. Dumas, and M.E. Whelland, *Appl. Phys. Lett.* **81**, 1252 (2002).